Supporting Information for

A-D-A-D-A Structured Organic Semiconductor Liposomes for NIR-II Fluorescence Imaging and Surgical Navigation of Lymph Node Metastasis

Qian Jiang,[a] *Xuqing Ying,*[a] *Xufeng Lu,*[a] *Chunjie Wei,*[b] *Kaiye Fu,*[a] *Shaoliang Yan,*[b] *Zhifa Shen,*[b] Jiaxi Ru*[b] and Ganhua Guo*[a]*

[a] The Third People's Hospital Health Care Group of Cixi, Ningbo, 315000, P. R. China.

[b] Cixi Biomedical Research Institute, Key Laboratory of Laboratory Medicine, Ministry of Education, Zhejiang Provincial Key Laboratory of Medical Genetics, School of Laboratory Medicine and Life sciences, Wenzhou Medical University, Zhejiang, 325000, P. R. China.

*Corresponding author: E-mail address: shenzhifa@wmu.edu.cn (Zhifa Shen), rujiaxi@wmu.edu.cn (Jiaxi Ru) and guoganhua1@163.com (Ganhua Guo).

Experimental section

Materials and Instrumentation

Materials. All reagents and solvents were obtained commercially and used without further purification unless otherwise noted. BTP-IC-OD, Y6 was purchased from Suna Tech Inc. DSPC, cholesterol (Chol), and DSPE-PEG_{2000}-FA were obtained from Ruixibio (China). 1 % Intralipid were purchased from Sigma-Aldrich (USA). PBS was purchased from Solarbio (China). CellTiter 96® AQueous One Solution Cell Proliferation Assay (MTS) was purchased from Promega (USA). CT26 cell lines was originally sourced from the American Type Culture Collection (ATCC). Female Balb/c mice were purchased from Beijing Weitong Lihua Experimental Animal Technology Co., Ltd.

Measurements. UV-vis absorption spectra were conducted on a UV-3210PC spectrophotometer. NIR-II fluorescence emission spectra were measured on Horiba Fluorolog-QM spectrophotometer equipped with a liquid-nitrogen-cooled InGaAs near-infrared array detector under ambient atmosphere. The cell viability assay was recorded using a SpectraMax 190 microplate reader (Molecular Devices). Liposome particle size and zeta potential were measured using a Litesizer DLS 500 dynamic light scattering instrument. *In vitro* and *in vivo* NIR-II fluorescence imaging was performed using the Mars ARTEMIS intelligent imaging system.

Drug-loading capacity and encapsulation efficiency

Prior to the encapsulation study, a calibration curve for the free **BTP-IC-OD** was constructed using UV-Vis spectroscopy at 752 nm (Fig. S1). To determine the encapsulation efficiency (EE%) and drug loading capacity (DL%), the liposomal formulation was subjected to ultracentrifugation to separate the encapsulated drug from the free drug. Specifically, the liposome suspension was centrifuged at 11,000 rpm for 5 minutes at 4°C. This process facilitated the sedimentation of the liposomal pellets, leaving the unencapsulated free **BTP-IC-OD** in the supernatant. Subsequently, the

supernatant was carefully collected, and the concentration of the free drug was quantified by measuring its absorbance against the pre-established calibration curve. All measurements were performed in triplicate.

Fluorescence quantum yields

Fluorescence quantum yields were measured by a relative method using IR26 in 1,2-dichloroethane (Φ_{std} = 0.05%) as the reference standard. UV-Vis-NIR absorption spectra were recorded on a UV-3210PC spectrophotometer, and NIR-II fluorescence emission spectra were obtained using a Horiba Fluorolog-QM fluorescence spectrometer. The quantum yield was calculated according to the following equation:

$$\Phi_u = \Phi_s \frac{D_u A_s n_u^2}{D_s A_u n_s^2}$$

where Φ is the quantum yield, D is the integrated area of the emission spectrum, A is the absorbance at the excitation wavelength, n is the refractive index of the solution, and the subscripts u and s refer to the unknown and the standard, respectively.

Supporting figures

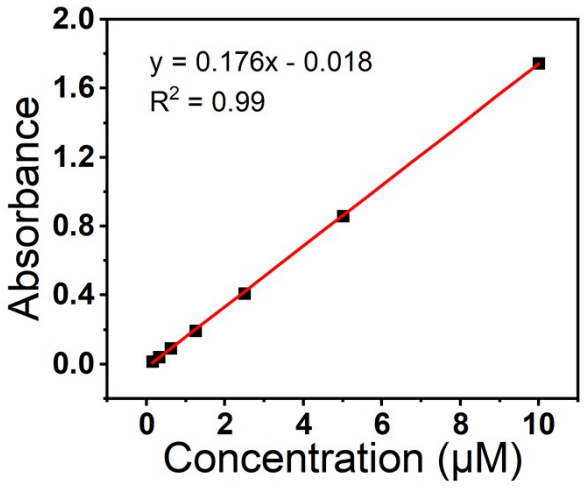

Fig. S1. Determination of the standard curve for free **BTP-IC-OD.**

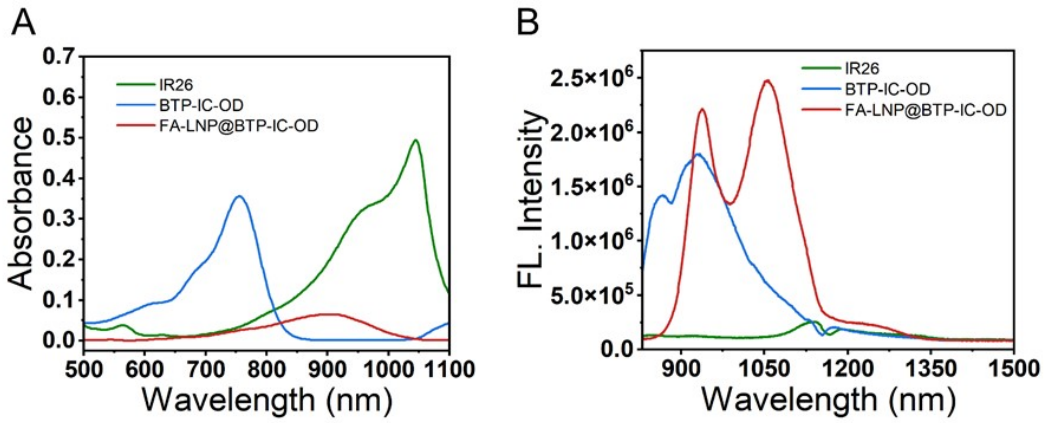

C

Sample	A_{808nm}	D	Solvent	n	Φ (%)
IR26	0.073	3.40×10^{7}	1,2-dichloroethane	1.45	0.05
BTP-IC-OD	0.097	3.18×10^{8}	CH_2Cl_2	1.42	0.46
FA-LNP@BTP-IC-OD	0.038	4.32×10^{8}	H_2O	1.33	1.04

Fig. S2. NIR-II fluorescence quantum yield characterization of BTP-IC-OD, FA-LNP@BTP-IC-OD, and IR26. (a) UV-Vis absorption spectra. (b) NIR-II fluorescence emission spectra. (c) Summary of fluorescence quantum yield (Φ) values and corresponding data.

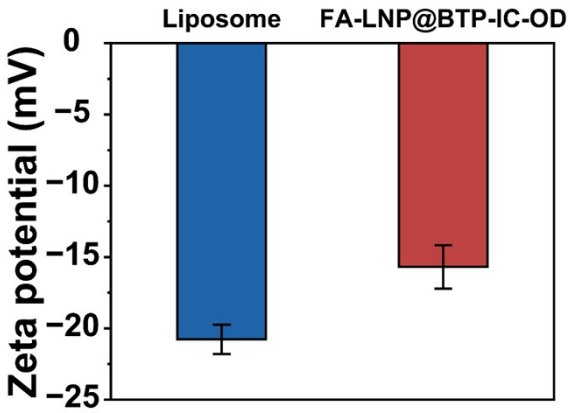

Fig. S3 Zeta potential of blank liposomes and **FA-LNP@BTP-IC-OD** in water.

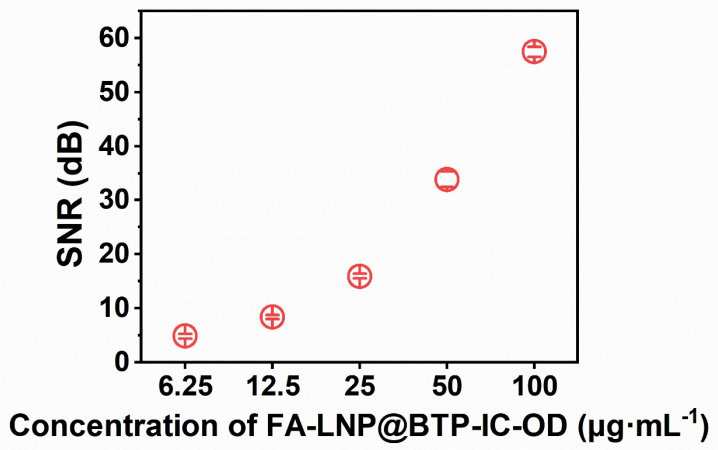

Fig. S4 The signal-to-noise ratio (SNR) of **FA-LNP@BTP-IC-OD** with different **BTP-IC-OD** concentrations in water.

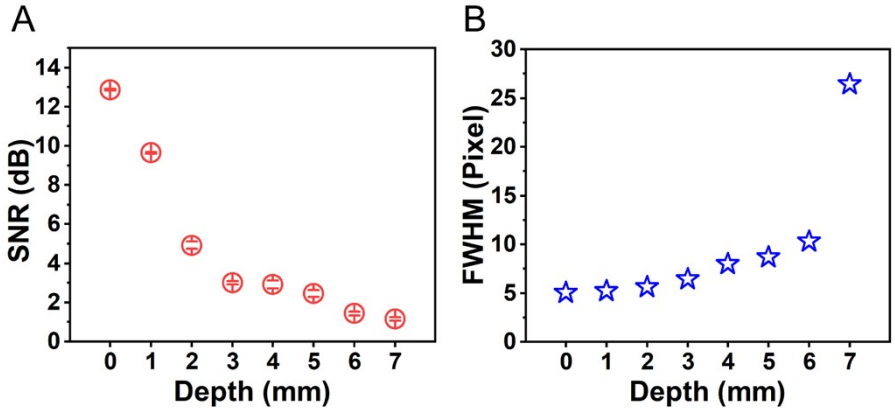

Fig. S5 The signal-to-noise ratio (SNR) and full width at half maximum (FWHM) of **FA-LNP@BTP-IC-OD** with a 1% intralipid coating at various thicknesses. (A) The SNR of **FA-LNP@BTP-IC-OD**. (B) The FWHM of **FA-LNP@BTP-IC-OD**.

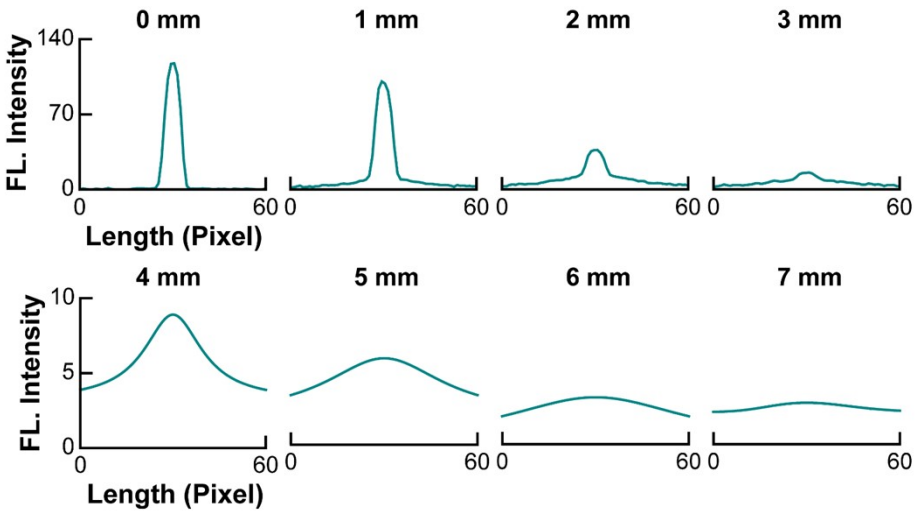

Fig. S6 The fluorescence intensity quantification of **FA-LNP@BTP-IC-OD** with variable intralipid coating thickness.

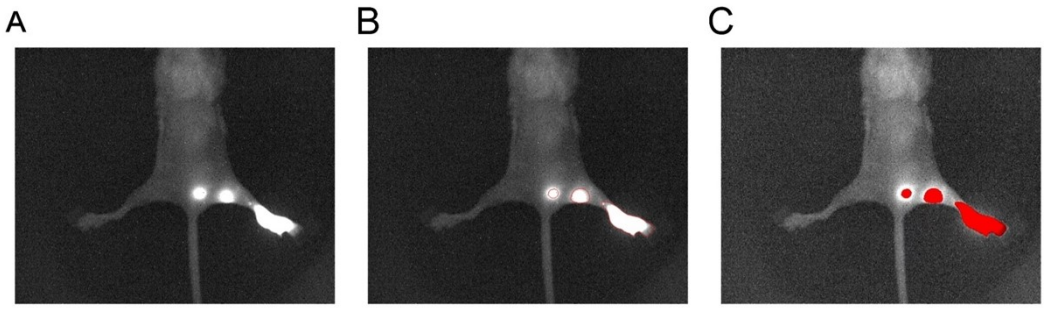

Figure S7 The NIR-II image segmentation with Cellpose SAM at 30 minutes post-injection. (A) The original NIR-II fluorescence image of the mouse acquired at 30 minutes post-injection. (B) The predicted outlines. (C) The predicted masks.

Supporting Table

Table S1. Determination of drug-loading capacity and encapsulation efficiency of **FA-LNP@BTP-IC-OD.**

No.	Free BTP-IC-OD (μg)	DL(%)	EE (%)
1	8.725	1.62	96.51
2	8.192	1.63	96.72
3	6.767	1.64	97.29